Magnetic Polymers for Microfluidic Sorting

Subjects: Polymer Science | Engineering, Biomedical

Contributor: Anne-laure Deman

Magnetophoresis offers many advantages for manipulating magnetic targets in microsystems. The integration of micro-flux concentrators and micro-magnets allows achieving large field gradients and therefore large reachable magnetic forces. However, the associated fabrication techniques are often complex and costly, and besides, they put specific constraints on the geometries. Magnetic composite polymers provide a promising alternative in terms of simplicity and fabrication costs, and they open new perspectives for the microstructuring, design, and integration of magnetic functions.

Keywords: magnetic polymers ; polymer composites ; magnetophoresis ; micro-bead separation ; cell separation ; microfluidic devices

1. Introduction

Microfluidics inspired vivid interest in biomedical applications as it meets a need for the manipulation of micro- and nanoscale objects by offering appealing features. Among them, we can cite: (i) its micrometric dimensions and laminar flow nature, enabling precise object manipulation and single-cell study; (ii) the handling of small quantities of volume, which facilitates the analysis of rare or expensive samples and speeds up processes, leading to cost-effective devices; (iii) the integration of various functions (mixing, focusing, sorting, trapping, detection, etc.) into a single device, leading to compact and portable systems and therefore opening the way for the implementation of point-of-care devices.

The manipulation of micro- and nano-objects requires external forces, such as acoustic, electrical, optical, or thermal actuations. In particular, magnetic forces are suitable for this purpose. Magnetic force-based manipulation relies on magnetophoresis, which refers to the motion of magnetic particles or magnetically labeled cells when subjected to a non-uniform magnetic field. Magnetophoresis [1][2][3][4][5] has been demonstrated as an efficient way to trap and separate biological entities, be it DNA [6][7][8], proteins [9][10][11], beads [12], or cells [13][14][15][16].

Composite polymers have recently emerged as a real breakthrough for the compatible and cost-effective integration of magnetic materials into polymer-based MEMS and microfluidic devices [17][18]. In general, the composite approach allows conferring new properties to the polymers and finds many applications in the field of smart devices [19]. Concerning magnetic composite polymers dedicated to microfluidic systems, this approach enables the tailoring of the magnetic function depending on the nature, the size, the concentration, and the morphology of the magnetic powder, the nature of the polymer matrix, and the microfabrication method. Various polymer materials have been investigated for microfluidic applications: elastomers such as polydimethylsiloxane (PDMS) [20], photosensitive resists such as SU-8 [21], or thermoplastics such as polymethylmethacrylate (PMMA) [22]. Magnetic PDMS is the most commonly encountered due to the microfabrication properties of PDMS by soft lithography and the massive use of the latter for the realization of microfluidic systems. Thus, a large panel of microfluidic functionalities for fluid sample handling has emerged employing composite polymers, such as micro-valves, micro-pumps, or micro-mixers for microfluidic flow control [17][21][23][24][25][26][27][28]; dynamic artificial cilia [22][29][30][31]; and reversible microchannel bonding [32]. Ferrofluids were also explored for actuation in microfluidic systems [33][34][35][36].

Magnetic polymers have also been used in microsystems to manipulate magnetic entities such as labeled cells or magnetic micro-beads by magnetophoresis. Several reviews published in the last few years show the richness of the literature and the vitality of magnetophoretic devices [37][38]. They also reveal that in their large majority, works are based on classical techniques of microelectronic manufacturing.

2. The PDMS Composite Approach

PDMS composites are excellent candidates for the integration of active functions into PDMS microsystems. There are many examples in the literature of dielectrophoretic functions based on conductive PDMS [39][40] and magnetic functions based on magnetic PDMS. Magnetic PDMS composites are mainly obtained by mixing soft (Fe, Ni, and Ni-Fe alloys) or

hard (NdFeB, ferrites) magnetic powders with a PDMS mixture (base polymer and curing agent). By modifying the nature, shape, concentration, and organization of the doping particles, it is possible to modulate the magnetic properties of the composite materials. One of the major advantages of these composites is that they preserve some properties of PDMS such as micropatterning by soft lithography and surface activation by O_2 for plasma bonding with glass and PDMS substrates. It also allows obtaining magnetic microstructures of several micrometers in thickness and with aspect ratios that are hardly obtained with conventional microfabrication techniques. In addition, the composite microstructure can be directly integrated into the microchannels, in a one-step soft-lithography process, avoiding tedious alignment procedures. This very versatile approach allows localizing the magnetic structures inside the channel or in its close vicinity, underneath or on the sides. Moreover, as the magnetic structures are integrated into PDMS microsystems, the polymer matrix being the same for the whole system, the magnetic function is tightly integrated and does not raise heterogeneous integration issues.

2.1. High Concentrated PDMS Composites

Bae et al. integrated pillar-like permanent micromagnets made from a mixture of a hard ferromagnetic powder, neodymium oxide (5 µm nominal diameter), and PDMS [41]. The magnetic powder and the PDMS were mixed before filling the molds. The molds of the circular pillars were realized with silanized PDMS. Nd-PDMS pillars of diameter ranging from 100 to 300 µm, and presenting a height of 240 µm, were obtained (**Figure 1**b). To convert the pillars into permanent magnets, they were magnetized with a magnetic field of 2.5 T. They implemented the array of pillars for immuno-magnetic separation using a streptavidin–biotin binding model of polymeric micro-beads and magnetic nanoparticles. Polymer micro-beads, 1 µm in diameter, were coated with streptavidin and magnetic nanoparticles (200 nm in diameter) with biotin. Capture efficiency of 94.9% was measured at 20 µL/min.

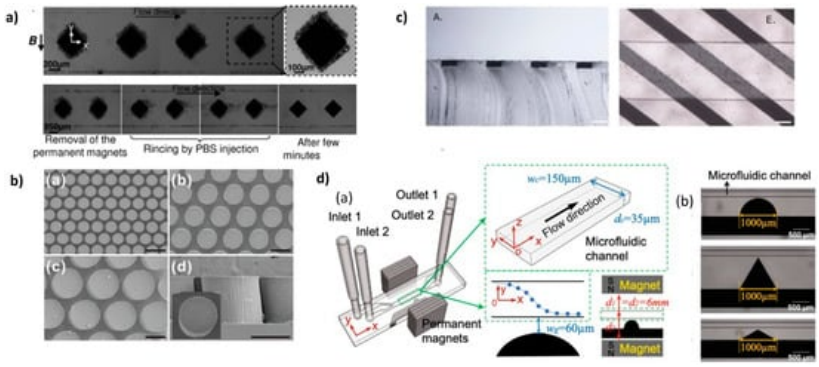

Figure 1. (**a**) Top: Capture of superparamagnetic beads suspended in PBS on several I-PDMS microstructures. The close-up allows distinguishing the beads trapped on a single structure. Bottom: Reversibility of the capture: the beads can be detached and collected by rinsing after removal of the magnets. Reprinted from [42], with the permission of AIP Publishing. (**b**) Scanning electron micrographs of 3D Nd-PDMS micropillar arrays of different diameters and inter-pillars distances. Scale bars: 200 µm. © IOP Publishing [41]. Reproduced with permission. All rights reserved. (**c**) Cross-sectional view of a PDMS flat slab with embedded soft magnetic stripes (A). Embedded strips on the bottom of the microfluidic chip (E). Scale bars: 100 µm. Reprinted from [43], with permission from Elsevier (**d**) (a) Schematic of the microsystem with the composite microstructure adjacent to the microfluidic channel. (b) Micro-photographies of the three different shapes for the composite microstructure next to the microfluidic channel: half circle, 60° isosceles triangle, and 120° isosceles triangle. Reprinted from [44] with permission.

2.2. High Concentrated PDMS Composites with Anisotropic Magnetic Properties

Deman et al. self-organized an 83 wt % (38 vol%) loaded I-PDMS (iron carbonyl/PDMS) composite by applying a 130 mT magnetic field during the polymer cross-linking step [45]. In the non-reticulated polymer, the motion of the magnetic entities is essentially driven by magnetic dipolar interactions. Depending on the relative positions of two adjacent magnetized particles, the interaction can be repulsive or attractive, which leads to anisotropic mechanisms of field-induced structures such as agglomeration and self-organization [46][47][48][49][50].

2.3. Low Concentrated PDMS Composites with Anisotropic Magnetic Properties

In contrast, when the volume fraction of the magnetic entities (particles [51][52], pillars [53][54], or fibers [55]) is reduced to few volume percentages, typically less than 10%, individual micrometer-sized magnetic flux sources can be formed and organized in regular patterns at the micrometer scale within the non-magnetic polymer matrix. To obtain well-organized arrays of micropatterns in PDMS, Le Roy et al. prepared micropillars on Si substrates topographically patterned by deep reactive ion etching and covered with 10 µm thick FeCo or NdFeB films. Then, the magnetic pillar arrays were transferred

in a PDMS membrane [56]. This approach offers a high quality of replication as well as a high control over the shape and the size of the magnetic structures. In turn, it involves advanced microfabrication processes for the deposition and the micropatterning.

As described previously for high concentrated composites, low concentrated composites are submitted to a magnetic field during the polymer cross-linking step. Thus, regular magnetic patterns of micrometric size and large aspect ratio can be obtained.

2.3.1. Preparation under Uniform Field

A uniform magnetic field induces a uniaxial symmetry in the dipolar interactions. These are attractive along the applied magnetic field direction but repulsive within the normal plane with respect to the applied field direction. Therefore, a uniform field promotes the formation of 1D agglomerates in the volume of the composite. **Figure 2** shows the microstructure and the magnetic properties of carbonyl iron particles/PDMS composite (I-PDMS) when prepared under a uniform magnetic field of 130 mT at different concentrations.

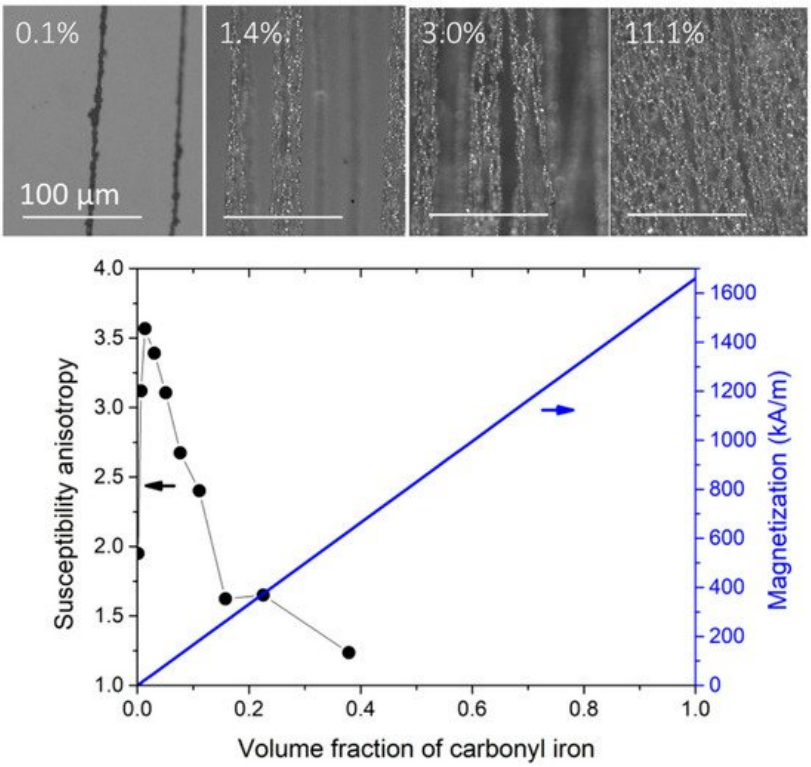

Figure 2. Anisotropic I-PDMS, prepared with an applied magnetic field of 130 mT. The top images are top views of I-PDMS membranes filled with volume concentrations of 0.1%, 1.4%, 3.0%, and 11.1% (from left to right). The columnar agglomerates are aligned in the direction of the applied magnetic field during the reticulation (vertical in the images). The graph shows the evolution of the anisotropy and the overall composite magnetization of the I-PDMS membranes. The susceptibility ratio is the ratio between the low field susceptibility in the direction of the applied field during the preparation and the in-plane perpendicular direction. Adapted with permission from [57] (http://creativecommons.org/licenses/by/4.0/).

An interesting feature of anisotropic I-PDMS is that it gives access, in its simplest implementation, to micro-patterns with interesting geometries (elongated patterns pointing toward the membrane's surface), which contrasts with standard micro-fabrication routes based on films. Mekkaoui et al. implemented I-PDMS, with carbonyl iron fraction of 1 and 5 wt % (0.13 and 0.68 vol %), in microfluidic devices [58] where the I-PDMS constitutes the channel's floor, exhibiting high densities of magnetic traps, of 1500 traps/mm^2 and 5000 traps/mm^2, for these two concentrations (**Figure 3**a).

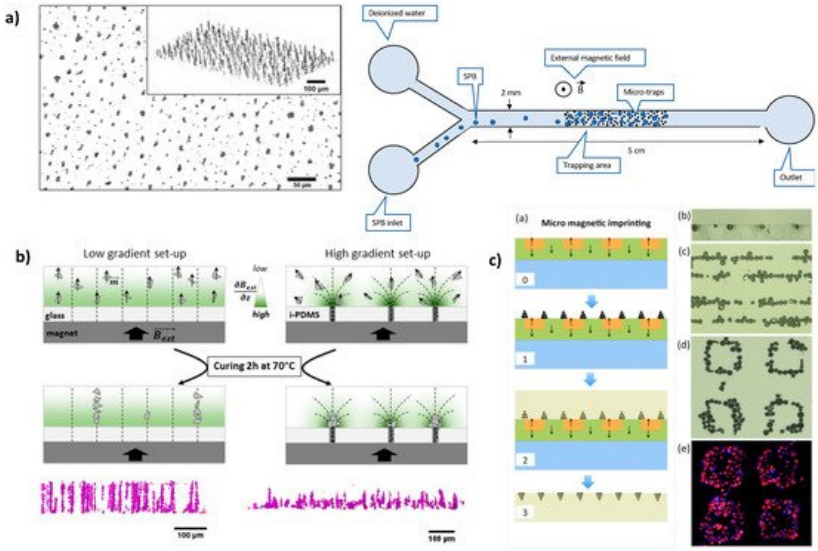

Figure 3. Examples of microstructure engineering by replication of a magnetic template. (**a**) X-ray tomography images of microstructured I-PDMS presenting arrays of columnar iron particle agglomerates. Adapted with permission from [58]. Copyright (2020) American Chemical Society. (**b**) Schematic views and X-ray tomography images of microstructured NdFeB@PDMS composite membranes prepared with two magnetic field patterns, leading to arrays of either columnar or conic agglomerates of NdFeB particles. Adapted with permission from [52]. (**c**) Fabrication scheme of NdFeB-PDMS membrane by micro-magnetic imprinting. Reprinted from [51] with permission of AIP Publishing.

2.3.2. Preparation under Magnetic Field Gradient

In the same aforementioned work, Descamps et al. compared the microstructure obtained with a uniform field and a non-uniform field applied during the crosslinking step [52]. In order to submit the composite layer to magnetic field gradients, they replaced the glass slide substrate with an I-PDMS membrane structured in an array of carbonyl iron-particle columns. The additional magnetic field template of the I-PDMS membrane led to a concentration of the NdFeB particles at the surface of the NdFeB-PDMS, forming arrays of conic agglomerates instead of columnar agglomerates (**Figure 3**b).

3. Magnetic Fluids

An external magnetic field magnetizes the ferrofluid (made of 17 vol% of 10 nm magnetite particles) and thus creates a gradient field (up to 1700 T/m) that attracts magnetic cells (macrophages containing phagocytosed magnetic nanoparticles and intrinsically magnetotactic bacteria) in the side channel (**Figure 4**a). Thus, the separation efficiency was 10 times increased compared to the separation with a magnet alone.

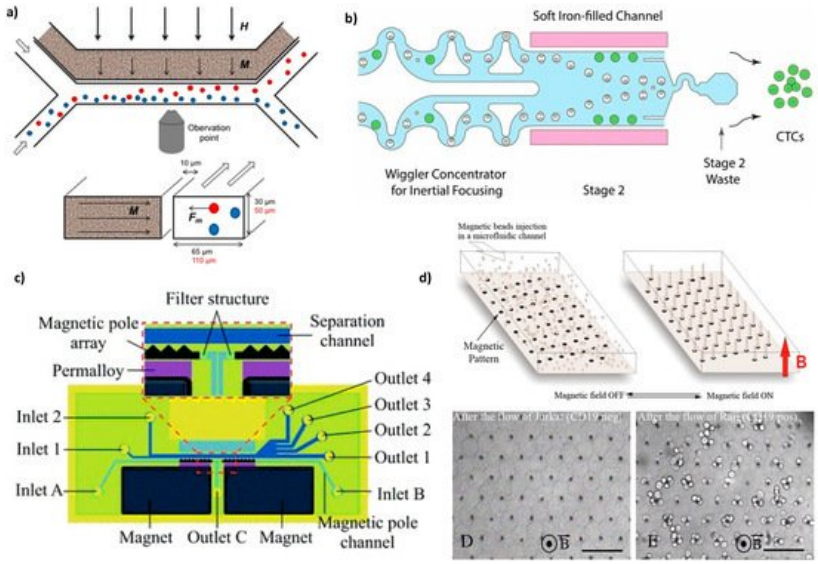

Figure 4. Microdevices with magnetically charged liquids used to trap or sort cells. (**a**) Design of the device seen from above (top) and as a cross-section through the channels (bottom). In the presence of an external magnetic field (thick arrows, H), the ferrofluid in the channel at 10 µm from the sorting channel magnetizes (thin arrows, M) and produces an attractive force (Fm) acting on magnetic cells (red), whereas non-magnetic cells (blue) continue in the sample flow. Reprinted from [59] with permission (http://creativecommons.org/licenses/by/4.0/). (**b**) Illustration of a magnetic sorter able

to deplete ≈3 billion WBCs (white blood cells) per hour from concentrated leukapheresis products. A first size-based inertial separation removes RBCs (red blood cells) and platelets. In stage 2, two channels, one on each side of the sorting channel are compactly packed with soft magnetic iron particles. Immunomagnetically labeled WBCs (white dots with beads) are deflected in the waste well 2, whereas CTCs (circulating tumor cells, green dots) are collected at the chip output. Reprinted from [60] with permission (http://creativecommons.org/licenses/by/4.0/). (**c**) Chip detail and an enlarged view of the separation region: the microfluidic structures are made of PDMS by soft lithography and bonded to a glass substrate, the magnetic pole arrays are filled with Fe_3O_4 powder, and the magnets are placed in opposite directions. Reprinted from [61], with the permission of the Royal Society of Chemistry (RSC). (**d**) Design of the Ephesia system (top): beads coated with an antibody are injected in a microchannel patterned with an array of magnetic ink, and the application of an external vertical magnetic field (red arrow) induces the formation of regular bead columns on top of the ink dots. Optical micrographs showing the application of the device (bottom): columns after the passage of 1000 Jurkat cells that exited the array (left) and columns after the passage of 400 Raji cells that were captured (right). Reprinted from [62] with permission of PNAS. Scale bars: 80 µm.

Recently, a more complex microfluidic system combined soft iron-filled channels to act as magnetic micro-concentrators to intensify the field gradient with a series of filters specifically designed to isolate CTC cells from magnetically labeled leukocytes [60] (**Figure 4**b).

Finally, a different approach is to use the self-organization properties of magnetic particles to produce magnetic traps inside the microfluidic channel. J. L. Viovy's group has been a pioneer in assembling biofunctionalized superparamagnetic beads (1 µm and 0.57 µm ± 5% of diameter) in a columnar organization to separate large DNA (from 10 to 160 kilobase pairs) [63][64]. Saliba et al. adapted this approach for micrometric objects, such as eukaryotic cells, by growing the magnetic columns of functionalized superparamagnetic beads onto a magnetic pattern obtained by microcontact printing of a water-based ferrofluid (a commercial magnetic ink) onto glass [62].

4. Conclusions

PDMS remains the most commonly employed polymer base in magnetic composites. However, thermoplastic polymers, such as polymehtylmethacrylate (PMMA), polycarbonate (PC), and cyclic olefin copolymer (COC), are commonly used in microfluidics and lab-on-a-chip devices [65][66] and may offer new avenues in the spread of magnetic polymer-based devices. In addition, micro-structured magnetic polymers in microfluidic devices are mainly performed by casting and soft lithography processes, but other printing methods, including 3D printing, are currently explored in soft electronics and soft robotics [67]. These cutting-edge techniques may be investigated by the microfluidic community to implement specific applications, including cell sorting.

References

1. Munaz, A.; Shiddiky, M.J.A.; Nguyen, N.T. Recent advances and current challenges in magnetophoresis based micro m agnetofluidics. Biomicrofluidics 2018, 12, 031501.
2. Luo, L.; He, Y. Magnetically driven microfluidics for isolation of circulating tumor cells. Cancer Med. 2020, 9, 4207–423 1.
3. Deman, A.-L.; Le Roy, D. Magnetophoresis in Bio-Devices. In Engineering of Micro/Nano Biosystems; Springer: Singap ore, 2020; pp. 309–361.
4. Pamme, N. Magnetism and microfluidics. Lab Chip 2006, 6, 24–38.
5. Cao, Q.; Fan, Q.; Chen, Q.; Liu, C.; Han, X.; Li, L. Recent advances in manipulation of micro- and nano-objects with m agnetic fields at small scales. Mater. Horiz. 2020, 7, 638–666.
6. Hung, P.Y.; Jiang, P.S.; Lee, E.F.; Fan, S.K.; Lu, Y.W. Genomic DNA extraction from whole blood using a digital microflu idic (DMF) platform with magnetic beads. Microsyst. Technol. 2015, 23, 313–320.
7. Dias, T.M.; Cardoso, F.A.; Martins, S.A.M.; Martins, V.C.; Cardoso, S.; Gaspar, J.F.; Monteiro, G.; Freitas, P.P. Impleme nting a strategy for on-chip detection of cell-free DNA fragments using GMR sensors: A translational application in canc er diagnostics using ALU elements. Anal. Methods 2016, 8, 119–128.
8. Garbarino, F.; Minero, G.A.S.; Rizzi, G.; Fock, J.; Hansen, M.F. Integration of rolling circle amplification and optomagnet ic detection on a polymer chip. Biosens. Bioelectron. 2019, 142, 111485.

9. Bejhed, R.S.; Tian, B.; Eriksson, K.; Brucas, R.; Oscarsson, S.; Strömberg, M.; Svedlindh, P.; Gunnarsson, K. Magneto phoretic Transport Line System for Rapid On-Chip Attomole Protein Detection. Langmuir 2015, 31, 10296–10302.
10. Zirath, H.; Schnetz, G.; Glatz, A.; Spittler, A.; Redl, H.; Peham, J.R. Bedside Immune Monitoring: An Automated Immun oassay Platform for Quantification of Blood Biomarkers in Patient Serum within 20 Minutes. Anal. Chem. 2017, 89, 481 7–4823.
11. Gao, Y.; Huo, W.; Zhang, L.; Lian, J.; Tao, W.; Song, C.; Tang, J.; Shi, S.; Gao, Y. Multiplex measurement of twelve tum or markers using a GMR multi-biomarker immunoassay biosensor. Biosens. Bioelectron. 2019, 123, 204–210.
12. Gijs, M.A.M.; Lacharme, F.; Lehmann, U. Microfluidic applications of magnetic particles for biological analysis and catal ysis. Chem. Rev. 2010, 110, 1518–1563.
13. Fachin, F.; Spuhler, P.; Martel-Foley, J.M.; Edd, J.F.; Barber, T.A.; Walsh, J.; Karabacak, M.; Pai, V.; Yu, M.; Smith, K.; e t al. Monolithic Chip for High-throughput Blood Cell Depletion to Sort Rare Circulating Tumor Cells. Sci. Rep. 2017, 7, 1 –11.
14. Zhao, W.; Cheng, R.; Lim, S.H.; Miller, J.R.; Zhang, W.; Tang, W.; Xie, J.; Mao, L. Biocompatible and label-free separati on of cancer cells from cell culture lines from white blood cells in ferrofluids. Lab Chip 2017, 17, 2243–2255.
15. Cho, H.; Kim, J.; Jeon, C.W.; Han, K.H. A disposable microfluidic device with a reusable magnetophoretic functional su bstrate for isolation of circulating tumor cells. Lab Chip 2017, 17, 4113–4123.
16. McCloskey, K.E.; Chalmers, J.J.; Zborowski, M. Magnetic Cell Separation: Characterization of Magnetophoretic Mobilit y. Anal. Chem. 2003, 75, 6868–6874.
17. Gray, B.L. A Review of Magnetic Composite Polymers Applied to Microfluidic Devices. J. Electrochem. Soc. 2014, 161, B3173–B3183.
18. Yunas, J.; Mulyanti, B.; Hamidah, I.; Said, M.M.; Pawinanto, R.E.; Wan Ali, W.A.F.; Subandi, A.; Hamzah, A.A.; Latif, R.; Majlis, B.Y. Polymer-Based MEMS electromagnetic actuator for biomedical application: A review. Polymers 2020, 12, 1 184.
19. Thévenot, J.; Oliveira, H.; Sandre, O.; Lecommandoux, S. Magnetic responsive polymer composite materials. Chem. S oc. Rev. 2013, 42, 7099–7116.
20. Li, J.; Zhang, M.; Wang, L.; Li, W.; Sheng, P.; Wen, W. Design and fabrication of microfluidic mixer from carbonyl iron-P DMS composite membrane. Microfluid. Nanofluidics 2011, 10, 919–925.
21. Nakahara, T.; Suzuki, J.; Hosokawa, Y.; Shimokawa, F.; Kotera, H.; Suzuki, T. Fabrication of Magnetically Driven Microv alve Arrays Using a Photosensitive Composite. Magnetochemistry 2018, 4, 7.
22. Currie, C.E.; Gray, B.L. Bidirectional Magnetic Polymer Membrane Actuators Integrated into Thermoplastic Microfluidic s. In Proceedings of the 2020 IEEE 33rd International Conference on Micro Electro Mechanical Systems (MEMS), Vanc ouver, BC, Canada, 18–22 January 2020; pp. 1056–1059.
23. Gholizadeh, A.; Javanmard, M. Magnetically Actuated Microfluidic Transistors: Miniaturized Micro-Valves Using Magnet orheological Fluids Integrated with Elastomeric Membranes. J. Microelectromech. Syst. 2016, 25, 922–928.
24. Paknahad, A.A.; Tahmasebipour, M. An electromagnetic micro-actuator with PDMS-Fe3O4 nanocomposite magnetic m embrane. Microelectron. Eng. 2019, 216, 111031.
25. Said, M.M.; Yunas, J.; Bais, B.; Hamzah, A.A.; Majlis, B.Y. The design, fabrication, and testing of an electromagnetic mi cropump with a matrix-patterned magnetic polymer composite actuator membrane. Micromachines 2017, 9, 13.
26. Nakahara, T.; Ueda, Y.; Miyagawa, H.; Kotera, H.; Suzuki, T. Self-aligned fabrication process for active membrane in m agnetically driven micropump using photosensitive composite. J. Micromech. Microeng. 2020, 30, 025006.
27. Zhou, R.; Surendran, A.N.; Mejulu, M.; Lin, Y. Rapid microfluidic mixer based on ferrofluid and integrated microscale nd feb-pdms magnet. Micromachines 2020, 11, 29.
28. Tang, S.Y.; Zhang, X.; Sun, S.; Yuan, D.; Zhao, Q.; Yan, S.; Deng, L.; Yun, G.; Zhang, J.; Zhang, S.; et al. Versatile Micr ofluidic Platforms Enabled by Novel Magnetorheological Elastomer Microactuators. Adv. Funct. Mater. 2018, 28, 1–10.
29. Rahbar, M.; Shannon, L.; Gray, B.L. Microfluidic active mixers employing ultra-high aspect-ratio rare-earth magnetic na no-composite polymer artificial cilia. J. Micromech. Microeng. 2014, 24, 025003.
30. Zhang, S.; Cui, Z.; Wang, Y.; Den Toonder, J.M.J. Metachronal actuation of microscopic magnetic artificial cilia generat es strong microfluidic pumping. Lab Chip 2020, 20, 3569–3581.
31. Zhang, S.; Zhang, R.; Wang, Y.; Onck, P.R.; Den Toonder, J.M.J. Controlled Multidirectional Particle Transportation by Magnetic Artificial Cilia. ACS Nano 2020, 14, 10313–10323.

32. Tsao, C.W.; Lee, Y.P. Magnetic microparticle-polydimethylsiloxane composite for reversible microchannel bonding. Sci. Technol. Adv. Mater. 2016, 17, 2–11.

33. Ashouri, M.; Shafii, M.B.; Moosavi, A. Theoretical and experimental studies of a magnetically actuated valveless microp ump. J. Micromech. Microeng. 2017, 27, 015016.

34. Hsu, M.C.; Alfadhel, A.; Forouzandeh, F.; Borkholder, D.A. Biocompatible magnetic nanocomposite microcapsules as m icrofluidic one-way diffusion blocking valves with ultra-low opening pressure. Mater. Des. 2018, 150, 86–93.

35. Luo, Z.; Evans, B.A.; Chang, C.H. Magnetically Actuated Dynamic Iridescence Inspired by the Neon Tetra. ACS Nano 2 019, 13, 4657–4666.

36. Luo, Z.; Zhang, X.A.; Evans, B.A.; Chang, C.H. Active Periodic Magnetic Nanostructures with High Aspect Ratio and Ult rahigh Pillar Density. ACS Appl. Mater. Interfaces 2020, 12, 11135–11143.

37. Lim, B.; Vavassori, P.; Sooryakumar, R.; Kim, C. Nano/micro-scale magnetophoretic devices for biomedical application s. J. Phys. D Appl. Phys. 2017, 50, 033002.

38. Alnaimat, F.; Karam, S.; Mathew, B.; Mathew, B. Magnetophoresis and Microfluidics: A Great Union. IEEE Nanotechnol. Mag. 2020, 14, 24–41.

39. Niu, X.; Peng, S.; Liu, L.; Wen, W.; Sheng, P. Characterizing and patterning of PDMS-based conducting composites. Ad v. Mater. 2007, 19, 2682–2686.

40. Deman, A.L.; Brun, M.; Quatresous, M.; Chateaux, J.F.; Frenea-Robin, M.; Haddour, N.; Semet, V.; Ferrigno, R. Charac terization of C-PDMS electrodes for electrokinetic applications in microfluidic systems. J. Micromech. Microeng. 2011, 2 1, 095013.

41. Bae, Y.M.; Jeong, B.; Kim, J.I.; Kang, D.G.; Shin, K.Y.; Yoo, D.W. Array of 3D permanent micromagnet for immunomagn etic separation. J. Micromech. Microeng. 2019, 29, 085007.

42. Faivre, M.; Gelszinnis, R.; Terrier, N.; Ferrigno, R.; Deman, A. Magnetophoretic manipulation in microsystem using carb onyl iron-polydimethylsiloxane microstructures. Biomicrofluidics 2014, 8, 054103.

43. Royet, D.; Hériveaux, Y.; Marchalot, J.; Scorretti, R.; Dias, A.; Dempsey, N.M.; Bonfim, M.; Simonet, P.; Frénéa-Robin, M. Using injection molding and reversible bonding for easy fabrication of magnetic cell trapping and sorting devices. J. Magn. Magn. Mater. 2017, 427, 306–313.

44. Zhou, R.; Wang, C. Microfluidic separation of magnetic particles with soft magnetic microstructures. Microfluid. Nanoflui dics 2016, 20, 1–11.

45. Deman, A.L.; Mekkaoui, S.; Dhungana, D.; Chateaux, J.F.; Tamion, A.; Degouttes, J. Dupuis, V.; Le Roy, D. Anisotropic composite polymer for high magnetic force in microfluidic systems. Microfluid. Nanofluidics 2017, 21, 170.

46. Liu, J.; Lawrence, E.M.; Wu, A.; Ivey, M.L.; Flores, G.A.; Javier, K.; Bibette, J.; Richard, J. Field-induced structures in fe rrofluid emulsions. Phys. Rev. Lett. 1995, 74, 2828–2831.

47. Martin, J.E.; Venturini, E.; Odinek, J.; Anderson, R.A. Anisotropic magnetism in field-structured composites. Phys. Rev. E Stat. Phys. Plasmas Fluids Relat. Interdiscip. Top. 2000, 61, 2818–2830.

48. Bertoni, G.; Torre, B.; Falqui, A.; Fragouli, D.; Athanassiou, A.; Cingolani, R. Nanochains formation of superparamagneti c nanoparticles. J. Phys. Chem. C 2011, 115, 7249–7254.

49. Wang, M.; He, L.; Yin, Y. Magnetic field guided colloidal assembly. Mater. Today 2013, 16, 110–116.

50. Ghosh, S.; Puri, I.K. Changing the magnetic properties of microstructure by directing the self-assembly of superparama gnetic nanoparticles. Faraday Discuss. 2015, 181, 423–435.

51. Dempsey, N.M.; Le Roy, D.; Marelli-Mathevon, H.; Shaw, G.; Dias, A.; Kramer, R.B.G.; Viet Cuong, L.; Kustov, M.; Zani ni, L.F.; Villard, C.; et al. Micro-magnetic imprinting of high field gradient magnetic flux sources. Appl. Phys. Lett. 2014, 104, 262401.

52. Descamps, L.; Mekkaoui, S.; Audry, M.-C.; Deman, A.-L.; Le Roy, D. Optimized process for the fabrication of PDMS me mbranes integrating permanent micro-magnet arrays. AIP Adv. 2020, 10, 15215.

53. Mitrossilis, D.; Röper, J.C.; Le Roy, D.; Driquez, B.; Michel, A.; Ménager, C.; Shaw, G.; Le Denmat, S.; Ranno, L.; Dum as-Bouchiat, F.; et al. Mechanotransductive cascade of Myo-II-dependent mesoderm and endoderm invaginations in e mbryo gastrulation. Nat. Commun. 2017, 8, 13883.

54. Bidan, C.M.; Fratzl, M.; Coullomb, A.; Moreau, P.; Lombard, A.H.; Wang, I.; Balland, M.; Boudou, T.; Dempsey, N.M.; D evillers, T.; et al. Magneto-active substrates for local mechanical stimulation of living cells. Sci. Rep. 2018, 8, 1–13.

55. Ourry, L.; Le Roy, D.; Mekkaoui, S.; Douillard, T.; Deman, A.L.; Salles, V. Magnetic filaments for anisotropic composite polymers. Nanotechnology 2020, 31, 9.

56. Le Roy, D.; Shaw, G.; Haettel, R.; Hasselbach, K.; Dumas-Bouchiat, F.; Givord, D.; Dempsey, N.M. Fabrication and cha racterization of polymer membranes with integrated arrays of high performance micro-magnets. Mater. Today Commun. 2016, 6, 50–55.
57. Le Roy, D.; Dhungana, D.; Ourry, L.; Faivre, M.; Ferrigno, R.; Tamion, A.; Dupuis, V.; Salles, V.; Deman, A.L. Anisotropi c ferromagnetic polymer: A first step for their implementation in microfluidic systems. AIP Adv. 2016, 6, 056604.
58. Mekkaoui, S.; Descamps, L.; Audry, M.; Deman, A.; Le Roy, D. Nanonewton Magnetophoretic Microtrap Array for Micro systems. Langmuir 2020, 36, 14546–14553.
59. Myklatun, A.; Cappetta, M.; Winklhofer, M.; Ntziachristos, V.; Westmeyer, G.G. Microfluidic sorting of intrinsically magne tic cells under visual control. Sci. Rep. 2017, 7, 1–8.
60. Mishra, A.; Dubash, T.D.; Edd, J.F.; Jewett, M.K.; Garre, S.G.; Karabacak, N.M.; Rabe, D.C.; Mutlu, B.R.; Walsh, J.R.; Kapur, R.; et al. Ultrahigh-throughput magnetic sorting of large blood volumes for epitope-agnostic isolation of circulatin g tumor cells. Proc. Natl. Acad. Sci. USA 2020, 117, 16839–16847.
61. Zeng, L.; Chen, X.; Du, J.; Yu, Z.; Zhang, R.; Zhang, Y.; Yang, H. Label-free separation of nanoscale particles by an ultr ahigh gradient magnetic field in a microfluidic device. Nanoscale 2021, 13, 4029.
62. Saliba, A.-E.; Saias, L.; Psychari, E.; Minc, N.; Simon, D.; Bidard, F.-C.; Mathiot, C.; Pierga, J.-Y.; Fraisier, V.; Salamer o, J.; et al. Microfluidic sorting and multimodal typing of cancer cells in self-assembled magnetic arrays. Proc. Natl. Aca d. Sci. USA 2010, 107, 14524–14529.
63. Doyle, P.S.; Bibette, J.; Bancaud, A.; Viovy, J.-L. Self-Assembled Magnetic Matrices for DNA Separation Chips. Science 2002, 295, 2237.
64. Minc, N.; Fütterer, C.; Dorfman, K.D.; Bancaud, A.; Gosse, C.; Goubault, C.; Viovy, J.L. Quantitative microfluidic separa tion of DNA in self-assembled magnetic matrixes. Anal. Chem. 2004, 76, 3770–3776.
65. Tsao, C.W. Polymer microfluidics: Simple, low-cost fabrication process bridging academic lab research to commercializ ed production. Micromachines 2016, 7, 225.
66. Gencturk, E.; Mutlu, S.; Ulgen, K.O. Advances in microfluidic devices made from thermoplastics used in cell biology an d analyses. Biomicrofluidics 2017, 11, 051502.
67. Kim, Y.; Yuk, H.; Zhao, R.; Chester, S.A.; Zhao, X. Printing ferromagnetic domains for untethered fast-transforming soft materials. Nature 2018, 558, 274–279.
